

Synthesis, Crystal Structures and Magnetism of a Series of Heptanuclear Rare-Earth-Centered Trigonal Prism Clusters

Qin-De Liu,^[a] Jun-Ran Li,^{*,[a]} Song Gao,^{*,[a]} Bao-Qing Ma,^[a] Hui-Zhong Kou,^[a]
Liang Ouyang,^[a] Rui-Li Huang,^[b] Xi-Xiang Zhang,^[c] and Kai-Bei Yu^[d]

Keywords: Copper / Lanthanides / N ligands / O ligands / Template synthesis / Magnetic properties

A series of heptanuclear rare-earth-centered trigonal prism clusters $[\text{LnCu}_6(\mu\text{-OH})_3(\text{HL})_2(\text{L})_4]\cdot(\text{ClO}_4)_2\cdot 25\text{H}_2\text{O}$ ($\text{Ln} = \text{La-Ho}$ and Y ; $\text{H}_2\text{L} = \text{iminodiacetic acid}$) was synthesized and their crystal structures were determined by X-ray diffraction. The rare-earth center and the copper ions are bridged by three $\mu_3\text{-OH}$ and six $\mu_2\text{-O}$ moieties from the carboxyl groups of six different ligands. The rare earth ion is nine-coordinate and the coordination polyhedron is an unusual, highly symmetrical tricapped trigonal prism (C_{3h}). The cluster has an interesting, highly symmetrical eclipsed structure (C_{3h})

which utilizes the central rare earth cation as a template. The temperature-dependence of the magnetic susceptibility of the cluster series was investigated and was found to vary with the central rare-earth ions. The magnitude of the anti-ferromagnetic interaction constants J between Cu^{2+} ions in $[\text{LaCu}_6]$ and $[\text{YCu}_6]$ were compared and estimated to be -24 cm^{-1} and -7 cm^{-1} , respectively, indicating a significant effect of the central diamagnetic ions.

(© Wiley-VCH Verlag GmbH & Co. KGaA, 69451 Weinheim, Germany, 2003)

Introduction

Heteronuclear transition-metal and rare-earth mixed complexes are of great interest due to their interesting structures and magnetic properties.^[1–9] These compounds are very important in understanding the nature of magnetic exchange interactions between rare-earth and transition-metal ions. Potential applications can be found for them in magnetic materials.^[2–8] However, previous magnetic investigations of these complexes have mostly focused on the nature of Gd–Cu coupling. Up until now, reports on Ln–Cu complexes other than those of Gd have been rather scarce.^[6,10–13] Whereas magnetostructural correlations have been established in some transition-metal complexes,^[14–21] little is known about the same correlation in polynuclear complexes containing both rare-earth and transition-metal ions.

Host-guest interactions have proven to be of paramount importance for the template synthesis of large magnetic clusters,^[22–25] and one expects to learn more on how the guests influence the magnetic coupling in the clusters. Schröder and co-workers reported some heteronuclear complexes obtained by template assembly of metal aggregates using imino-carboxylate ligands.^[26] In that work, a tetradentate ligand was used to synthesize complexes that contained various metal ions as templates. Recently we reported the structures and magnetic properties of $[\text{LaCu}_6]$ and $[\text{TbCu}_6]$ clusters.^[13] As an extension of that work, a series of heptanuclear lanthanide-centered trigonal prism clusters $[\text{LnCu}_6(\mu\text{-OH})_3(\text{HL})_2(\text{L})_4]\cdot(\text{ClO}_4)_2\cdot 25\text{H}_2\text{O}$ ($\text{Ln} = \text{Ce-Gd}$, Dy-Ho and Y ; $\text{H}_2\text{L} = \text{iminodiacetic acid}$), were obtained at a considerably higher pH value (approx. 6.0), and their magnetic behaviors were studied in the context of their structures.

Results and Discussion

IR Spectra

Using $[\text{GdCu}_6]$ as an example, the IR resonances of the carboxylate moiety, $\nu_{\text{as}}(\text{OCO})$ and $\nu_{\text{s}}(\text{OCO})$, in free (H_2L) and coordinated (HL) ligands were compared. After coordination to the metal centers, the $\nu_{\text{as}}(\text{OCO})$ absorption was found to have blue-shifted 45 cm^{-1} , from a value of 1583 cm^{-1} to 1628 cm^{-1} ; the $\nu_{\text{s}}(\text{OCO})$ absorption at 1397 cm^{-1} shifted 35 cm^{-1} up to 1432 cm^{-1} , and 19 cm^{-1}

^[a] State Key Laboratory of Rare Earth Materials Chemistry and Applications, PKU-HKU Joint Laboratory on Rare Earth Materials and Bioinorganic Chemistry, College of Chemistry and Molecular Engineering, Peking University, Beijing 100871, China
E-mail: lijunran@pku.edu.cn; gaosong@pku.edu.cn

^[b] Department of Chemistry, Iowa State University, USA

^[c] Department of Physics, The Hong Kong University of Science and Technology, Clear Water Bay, Kowloon, Hong Kong

^[d] Chengdu Center for Analysis and Measurement, Academia Sinica, Chengdu 610041, China

down to 1378 cm^{-1} . This shows that the two carboxyl groups of the ligand bound to the metal ions have two coordination modes.^[26] The value of $\nu_s(\text{C}-\text{N})$ in the complex shifted 92 cm^{-1} down to 1118 cm^{-1} . These results indicate that the carboxyl groups and the N atom of the ligand are all coordinated to metal ions. The IR spectra of the other $[\text{LnCu}_6]$ complexes are very similar to that of $[\text{GdCu}_6]$.

Thermal Analysis

The thermal behavior of all eleven complexes is similar. For example, the crystalline compound $[\text{GdCu}_6]$ begins to lose part of its crystal lattice water molecules at a surprisingly low temperature (around $30\text{ }^\circ\text{C}$), and the water-loss rate reaches a maximum at ca $56\text{ }^\circ\text{C}$. The complex loses a total of nine water molecules in the temperature range $30.0\text{--}60.0\text{ }^\circ\text{C}$ (loss of weight found: 8.1% ; loss of weight calculated based on the loss of nine water molecules: 8.0%). The thermal analysis results are in accordance with the elemental analysis results for all eleven complexes. Elemental analysis data are given in Table 1.

Table 1. Elemental analysis data

	C (%)	Calcd. (found) H (%)	N (%)
$\text{C}_{24}\text{H}_{67}\text{Cl}_2\text{Cu}_6\text{LaN}_6\text{O}_{51}$	15.61 (15.27)	3.66 (3.45)	4.55 (4.57)
$\text{C}_{24}\text{H}_{67}\text{CeCl}_2\text{Cu}_6\text{N}_6\text{O}_{51}$	15.60 (15.67)	3.65 (3.60)	4.55 (4.53)
$\text{C}_{24}\text{H}_{67}\text{Cl}_2\text{Cu}_6\text{N}_6\text{O}_{51}\text{Pr}$	15.59 (15.67)	3.65 (3.70)	4.55 (4.62)
$\text{C}_{24}\text{H}_{67}\text{Cl}_2\text{Cu}_6\text{N}_6\text{NdO}_{51}$	15.56 (15.83)	3.65 (3.84)	4.54 (4.53)
$\text{C}_{24}\text{H}_{67}\text{Cl}_2\text{Cu}_6\text{N}_6\text{O}_{51}\text{Sm}$	15.51 (15.89)	3.63 (3.58)	4.52 (4.56)
$\text{C}_{24}\text{H}_{67}\text{Cl}_2\text{Cu}_6\text{EuN}_6\text{O}_{51}$	15.50 (15.57)	3.63 (3.53)	4.52 (4.57)
$\text{C}_{24}\text{H}_{67}\text{Cl}_2\text{Cu}_6\text{GdN}_6\text{O}_{51}$	15.45 (15.53)	3.62 (3.61)	4.51 (4.70)
$\text{C}_{24}\text{H}_{67}\text{Cl}_2\text{Cu}_6\text{N}_6\text{O}_{51}\text{Tb}$	15.44 (15.00)	3.62 (3.21)	4.50 (4.32)
$\text{C}_{24}\text{H}_{67}\text{Cl}_2\text{Cu}_6\text{DyN}_6\text{O}_{51}$	15.41 (15.49)	3.61 (3.56)	4.49 (4.48)
$\text{C}_{24}\text{H}_{67}\text{Cl}_2\text{Cu}_6\text{HoN}_6\text{O}_{51}$	15.39 (15.42)	3.61 (3.67)	4.49 (4.71)
$\text{C}_{24}\text{H}_{67}\text{Cl}_2\text{Cu}_6\text{N}_6\text{O}_{51}\text{Y}$	16.04 (16.36)	3.76 (3.71)	4.68 (4.90)

Description of Structures

X-ray diffraction analyses indicate that these complexes are isomorphous. Among them the crystal structures of the $[\text{LaCu}_6]$ and $[\text{TbCu}_6]$ complexes have been reported.^[13] As a typical example, the structural features of $[\text{SmCu}_6]$ will be discussed briefly. Figure 1 shows an ORTEP view of this complex. The Sm^{3+} ion is nine-coordinate and the coordination polyhedron can be described as a tricapped trigonal prism, which is highly symmetrical. The observed geometries of nine-coordinate lanthanide ions are usually asymmetrical monocapped square antiprism^[28,29] or distorted tricapped trigonal prism.^[30–32] This kind of highly symmetrical coordination polyhedron (C_{3h}) is very unusual among 4f-3d and 4f coordination compounds. The Cu^{2+} ions in the complex are all five-coordinate, exhibiting a distorted tetragonal pyramidal geometry. Crystal data, details of data collection, and refinement are listed in Table 2. Crystal cell parameters of all the complexes are listed in

Table 3 and important bond lengths and angles are given in Table 4.

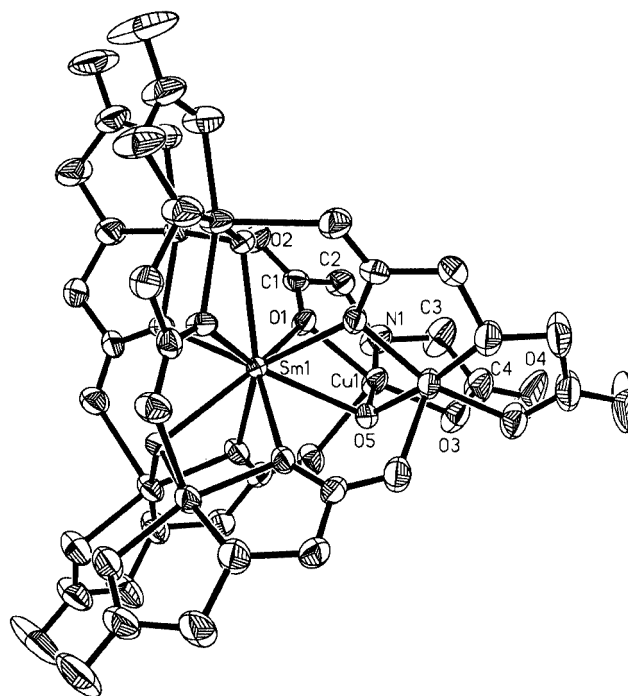


Figure 1. An ORTEP drawing of $[\text{SmCu}_6]$

The $[\text{SmCu}_6]$ cluster consists of two parallel layers, with each layer being composed of three Cu^{2+} ions and three L's. The six Cu^{2+} ions form a trigonal prism (C_{3h}) with the Sm^{3+} ion located in the center (Figure 2). The Sm^{3+} ion lying between two layers is bridged to the six Cu^{2+} ions by three $\mu_3\text{-OH}$ groups and six $\mu_2\text{-O}$ atoms from six L's. Therefore, the two layers are connected by the nine-coordinate Sm^{3+} ion and three $\mu_3\text{-OH}$ groups. Each $\mu_3\text{-OH}$ is coordinated to the Sm^{3+} ion and two Cu^{2+} ions, one from each layer.

The structural features of the eleven complexes are practically the same, except that the volumes of the crystal cells are slightly different. This result shows that almost all the rare earth ions (except for Er, Tm, Yb, and Lu) can be centered in this type of $[\text{LnCu}_6]$ complex. Crystals of these complexes were obtained at relatively high pH (approx. 6). Therefore, it can be considered that these complexes were assembled using a rare-earth cation as the template, and the process is also affected by the μ_3 -bridged hydroxyl groups yielded from the slow hydrolysis of the rare earth ions while the pH value of the reaction mixture was adjusted with aqueous ammonia. From their crystal cell parameters (Table 3), we can see that the size of the trigonal prism cage formed by Cu^{2+} ions does not change much in the presence of different rare earth ions. This indicates that the radius of the template cation should be limited to within a certain range. Our failure to obtain complexes of Er, Tm, Yb and Lu similar to $[\text{SmCu}_6]$ may be explained by the fact that the

Table 2 Crystallographic data for [SmCu₆] [GdCu₆] [HoCu₆] and [YCu₆]; space group *P*6₃/*m*

Empirical formula	C ₂₄ H ₈₅ Cl ₂ Cu ₆ N ₆ O ₆₀ Sm	C ₂₄ H ₈₅ Cl ₂ Cu ₆ GdN ₆ O ₆₀	C ₂₄ Cl ₂ Cu ₆ H ₈₅ HoN ₆ O ₆₀	C ₂₄ H ₈₅ Cl ₂ Cu ₆ N ₆ O ₆₀ Y
Color	blue	blue	blue	blue
Crystal size (mm)	0.25 × 0.23 × 0.17	0.48 × 0.38 × 0.30	0.30 × 0.30 × 0.20	0.31 × 0.25 × 0.19
Crystal system	Hexagonal	Hexagonal	Hexagonal	Hexagonal
Space group	<i>P</i> 6 ₃ / <i>m</i>	<i>P</i> 6 ₃ / <i>m</i>	<i>P</i> 6 ₃ / <i>m</i>	<i>P</i> 6 ₃ / <i>m</i>
<i>a</i> (Å)	12.6126(7)	12.6157(15)	12.587(2)	12.5840(18)
<i>b</i> (Å)	12.6126(7)	12.6157(15)	12.587(2)	12.5840(18)
<i>c</i> (Å)	24.4445(13)	24.415(6)	24.354(5)	24.415(5)
α (°)	90	90	90	90
β (°)	90	90	90	90
γ (°)	120	120	120	120
<i>V</i> (Å ³)	3367.6(3)	3365.2(10)	3341.5(10)	3348.3(10)
<i>Z</i>	2	2	2	2
<i>M</i>	2020.47	2027.36	2035.05	1959.02
<i>D_c</i> (g cm ^{−3})	1.993	2.001	2.023	1.973
Absorption coefficient (mm ^{−1})	2.931	3.039	3.246	2.940
<i>F</i> (000)	2042	2046	2052	1996
λ (Å) (Mo- <i>Kα</i>)	0.71073	0.71073	0.71073	0.71073
Monochromator	Graphite	Graphite	Graphite	Graphite
θ range for data collection (°)	1.67–28.33	2.04–25.00	2.05–25.01	3.64–25.00
Index range <i>h</i> ; <i>k</i> ; <i>l</i>	−11 to 16 −16 to 15 −32 to 32	0 to 14 −14 to 1 0 to 29	0 to 12 0 to 12 0 to 28	0 to 14 −12 to 0 −28 to 29
Reflections collected	23747	4587	2192	3909
Independent reflections	2870 (<i>R</i> _{int} = 7.78%)	2019 (<i>R</i> _{int} = 3.75%)	1919 (<i>R</i> _{int} = 6.55%)	2009 (<i>R</i> _{int} = 1.82%)
Observed reflections	2137 [<i>I</i> > 2 σ (<i>I</i>)]	1519 [<i>I</i> > 2 σ (<i>I</i>)]	1370 [<i>I</i> > 2 σ (<i>I</i>)]	1787 [<i>I</i> > 2 σ (<i>I</i>)]
Number of parameters refined	181	168	182	182
Final <i>R</i>	0.0588	0.0467	0.0487	0.0611
Final <i>wR</i>	0.1585	0.1246	0.1280	0.1676
Goodness-of-fit on <i>F</i> ²	1.055	0.966	1.038	1.040

Table 3. Crystal cell parameters of the [LnCu₆] complexes; space group *P*6₃/*m*

Complex	Color	Crystal system	<i>a</i> (Å)	<i>b</i> (Å)	<i>c</i> (Å)	α (°)	β (°)	γ (°)
[LaCu ₆]	blue	hexagonal	12.6425(14)	12.6425(14)	24.541(5)	90	90	120
[CeCu ₆]	blue	hexagonal	12.672(2)	12.672(2)	24.563(5)	90	90	120
[PrCu ₆]	blue	hexagonal	12.677(2)	12.677(2)	24.538(5)	90	90	120
[NdCu ₆]	blue	hexagonal	12.666(2)	12.666(2)	24.607(5)	90	90	120
[SmCu ₆]	blue	hexagonal	12.6126(7)	12.6126(7)	24.445(13)	90	90	120
[EuCu ₆]	blue	hexagonal	12.663(5)	12.663(5)	24.538(9)	90	90	120
[GdCu ₆]	blue	hexagonal	12.6157(15)	12.6157(15)	24.415(6)	90	90	120
[TbCu ₆]	blue	hexagonal	12.5802(9)	12.5802(9)	24.285(4)	90	90	120
[DyCu ₆]	blue	hexagonal	12.619(8)	12.619(8)	24.454(5)	90	90	120
[HoCu ₆]	blue	hexagonal	12.587(2)	12.587(2)	24.354(5)	90	90	120
[YCu ₆]	blue	hexagonal	12.584(2)	12.584(2)	24.415(4)	90	90	120

radii of these ions are too small for them to be stably centered in the cage.

Magnetic Properties

The temperature dependence of the magnetic susceptibilities (χ_M) and of $\chi_M T$ for [LaCu₆], [PrCu₆], [NdCu₆], [GdCu₆], [TbCu₆], [DyCu₆], [HoCu₆], and [YCu₆] are shown in Figure 3 and Figure 4. The M...M (M = Ln or Cu) distances in some [LnCu₆] clusters are listed in Table 5.

It can be seen that the complexes exhibit different overall magnetic behaviors which seem to be dependent upon the different central rare earth ions within the [LnCu₆] complexes, even though all these complexes are isomorphous. Our previous results tells us that the magnetic interactions

between the Cu²⁺ ions are antiferromagnetic in [LaCu₆], and there is a ferromagnetic coupling between the Tb³⁺ and Cu²⁺ ions in [TbCu₆].^[13] The magnetic behavior of [GdCu₆], which shows an obvious ferromagnetic coupling between the Gd³⁺ and Cu²⁺ ions, is similar to that of [TbCu₆]. Referring to the structural data in Table 5, the M...M separations in [GdCu₆] are all very similar to those in [TbCu₆] (with a general difference of ca 0.01 Å). This may be an explanation for their similar magnetic behavior. For [DyCu₆], [HoCu₆], [NdCu₆], and [PrCu₆], the nature of the magnetic interactions between the Ln³⁺ and Cu²⁺ ions cannot be definitively defined because the magnetic behavior of these systems can be affected by many factors, such as the Ln–Ln, Cu–Cu, and Ln–Cu interactions, the

Table 4. Selected bond lengths (Å) and angles (deg) for [SmCu₆], [GdCu₆], [HoCu₆] and [YCu₆]^[a]

	[SmCu ₆]	[GdCu ₆]	[HoCu ₆]	[YCu ₆]
Ln–O1	2.464(4)	2.457(4)	2.421(7)	2.425(4)
Ln–O5	2.495(6)	2.489(6)	2.445(11)	2.438(6)
Cu–O1	1.973(4)	1.980(4)	1.977(8)	1.977(4)
Cu–O3	1.933(5)	1.940(5)	1.937(9)	1.939(4)
Cu–O5	1.933(3)	1.935(3)	1.935(6)	1.935(3)
Cu–N	1.961(6)	1.970(6)	1.958(10)	1.980(6)
Cu–O2A	2.310(5)	2.294(5)	2.278(9)	2.279(4)
O1–Ln–O1A	75.8(2)	75.48(17)	76.0(3)	75.57(15)
O1–Ln–O1C	89.6(2)	90.1(2)	89.4(4)	89.9(2)
O1–Ln–O1E	138.43(8)	138.61(8)	138.36(14)	138.57(7)
O1–Ln–O5	65.66(14)	66.11(13)	66.3(2)	66.11(14)
O1–Ln–O5B	72.89(15)	72.59(14)	72.2(3)	72.55(14)
O1–Ln–O5A	134.94(11)	134.76(11)	135.13(19)	134.82(10)
O5–Ln–O5B	120.000(1)	120.000(1)	120.010(4)	120.000(1)
O1–Cu–N	85.5(2)	85.2(2)	85.5(4)	85.8(2)
O1–Cu–O3	163.7(2)	163.8(2)	163.8(4)	163.74(19)
O1–Cu–O5	87.0(2)	87.1(2)	85.7(4)	85.4(2)
O1–Cu–O2A	94.8(2)	94.76(18)	94.9(3)	94.79(17)
O3–Cu–N	85.0(2)	85.4(2)	85.6(4)	85.2(2)
O3–Cu–O5	101.7(2)	101.4(2)	102.5(4)	102.7(2)
O3–Cu–O2A	98.8(2)	98.8(2)	99.0(4)	99.00(19)
O5–Cu–N	172.0(3)	171.9(3)	171.1(5)	170.9(3)
O5–Cu–O2A	91.4(2)	91.0(2)	90.4(4)	91.6(2)
N–Cu–O2A	91.8(2)	92.2(3)	92.1(5)	91.5(2)
Cu–O1–Ln	102.3(2)	102.07(18)	102.6(3)	102.62(16)
Cu–O5–Ln	102.5(2)	102.30(19)	103.1(4)	103.5(2)
Cu–O5–CuC	119.4(3)	118.8(3)	117.3(5)	118.4(3)

[a] Symmetry transformations used to generate equivalent atoms: A $-y + 1, x - y + 1, z$; B $-x + y, -x + 1, z$; C $x, y, -z + 1/2$; D $-y + 1, x - y + 1, -z + 1/2$; E $-x + y, -x + 1, -z + 1/2$

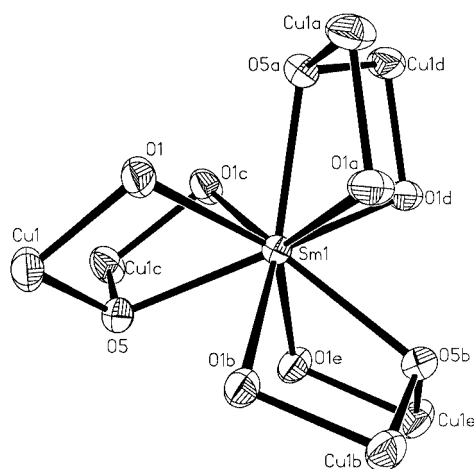


Figure 2. The trigonal prism cage formed by six Cu²⁺ and the bridges among Sm³⁺ and six Cu²⁺ (O5, O5C, O5E are from the three μ₃-OH; O1, O1A–O1E are from carboxyl groups of the six ligands)

ligand-field effects of the Ln³⁺ ion, and field saturation effects.

Figure 4 indicates that the interactions between the Cu²⁺ ions in [LaCu₆] and [YCu₆] are all antiferromagnetic in nature. However, the magnitudes of these antiferromagnetic interactions are different, and the *J* values are evaluated to

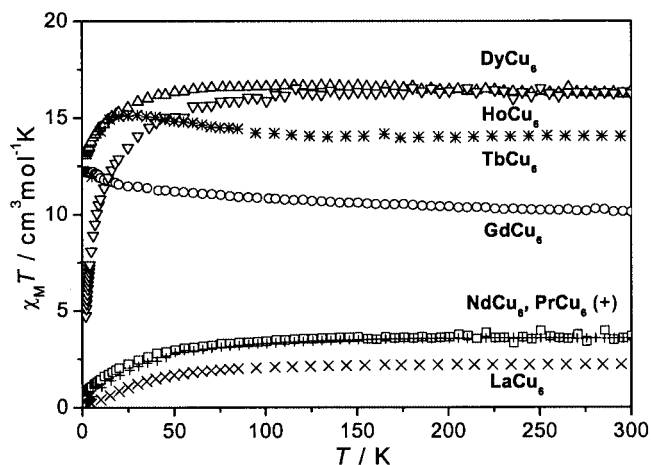


Figure 3. Plot of the magnetic susceptibilities (χ_M) and the $\chi_M T$ product vs. *T* for [LaCu₆], [PrCu₆], [NdCu₆], [GdCu₆], [TbCu₆], [DyCu₆], [HoCu₆]

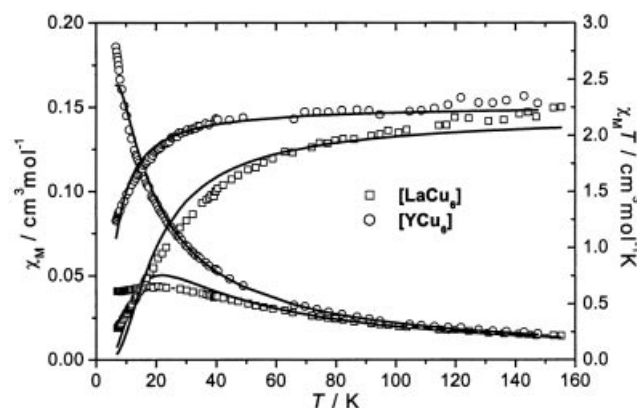


Figure 4. Plot of the magnetic susceptibilities (χ_M) and the $\chi_M T$ product vs. *T* for [LaCu₆] and [YCu₆]; solid lines show the best fit of the data

be -24 cm^{-1} and -7 cm^{-1} for [LaCu₆] and [YCu₆], respectively, using the same approach as previously^[13] ($R = \Sigma(\chi_M T^{\text{cal}} - \chi_M T^{\text{obs}})^2 / \Sigma(\chi_M T^{\text{obs}})^2 = 7.4 \times 10^{-3}$, and 9.7×10^{-4} for [LaCu₆] and [YCu₆], respectively). The difference in the *J* values shows the significant impact of the central diamagnetic ions, La³⁺ and Y³⁺. Upon substitution of La³⁺ ion with Y³⁺ ion, the Cu²⁺–Cu²⁺ distances decrease from 5.325 Å, 3.383 Å and 6.309 Å to 5.231 Å, 3.324 Å and 6.197 Å, the Ln³⁺–Cu²⁺ distance decreases from 3.509 Å to 3.447 Å, and the Cu²⁺–O–Cu²⁺ angle decreases from 120.7° to 118.4°. Therefore, the shorter ionic radius of Y³⁺ (1.075 Å), with respect to that of La³⁺ (1.216 Å), leads to a decrease in the size of the cage composed from the Cu²⁺ ions. The fact that the *J* value is larger in [LaCu₆] than in [YCu₆] reveals a dependency of *J* on the Cu²⁺–Cu²⁺ separation and the Cu²⁺–O–Cu²⁺ angle: smaller Cu²⁺–Cu²⁺ separations and Cu²⁺–O–Cu²⁺ angles lead to weaker antiferromagnetic exchange-coupling interactions between the Cu²⁺ ions for the systems in this paper. This result is consistent with the conclusion drawn previously,^[17] showing that the direct overlap of metal orbitals plays a minor role, since it would enhance

Table 5. Selected M...M distances (Å) and Cu–O–Cu angles (deg)

	Cu...Cu (intra-layer)	Cu...Cu (inter-layer)	Ln...Cu	Cu–O–Cu
[LaCu ₆]	5.325	3.383, 6.309	3.509	120.7
[SmCu ₆]	5.271	3.337, 6.238	3.470	119.4
[GdCu ₆]	5.258	3.331, 6.225	3.463	118.8
[TbCu ₆]	5.245	3.319, 6.207	3.453	118.1
[HoCu ₆]	5.233	3.304, 6.189	3.444	117.3
[YCu ₆]	5.231	3.324, 6.197	3.447	118.4

antiferromagnetic coupling at shorter Cu...Cu separations. The encapsulated Ln³⁺ ion in the cage has a tuning effect on the magnetism of the core: the magnetic behavior is related to the ionic radius of the guest rare earth ion, which determines the exact geometry of the bridging ligands.

Conclusion

A series of highly symmetrical heptanuclear trigonal prism clusters, [LnCu₆], was assembled using rare earth cations as templates. The process is also affected by the μ₃-bridged hydroxyl groups. It was also shown that different central rare-earth ions in the cage significantly influence the magnetic behavior of these complexes.

Experimental Section

Physical Measurements: Elemental analysis was performed on a German Elementar Vario EL instrument. IR spectra were measured as KBr pellets with a Nicolet Magna-IR 750 spectrometer at 295 K. Thermal analyses were performed on a Du Pont 1090B thermal analyzer. Magnetic measurements were performed on a SQUID and an Oxford MagLab2000 System in the temperature range 2–300 K. Diamagnetic corrections were estimated on the basis of Pascal's constants. All starting materials were analytical reagents from Beijing Reagent Co. Sodium iminodiacetate (Na₂L) was obtained by the direct reaction of iminodiacetic acid with sodium hydroxide in an aqueous solution.

Preparations

LnCu₆C₂₄H₈₅N₆Cl₂O₆₀ (Ln = La–Ho and Y): All heptanuclear complexes (La–Ho, Y) were synthesized by first mixing copper perchlorate, the rare earth perchlorate and sodium iminodiacetate (1:1:1 mol ratio) in 10 cm³ water under vigorous stirring, then carefully adjusting the pH value to about 6 with aqueous ammonia. The reaction mixture was left to stand at room temperature. After two days, deep-blue hexagonal prism crystals of LnCu₆C₂₄H₈₅N₆Cl₂O₆₀ (Ln = La–Ho and Y) were obtained and collected, with yields of ca 20%. Previous to the elemental analyses, the loosely bound waters of crystallization were eliminated by keeping the products at 60 °C until constant weights were reached. The results of elemental analysis are listed in Table 1. Similar crystals of the compounds with Ln = Er, Tm, Yb or Lu could not be obtained.

X-ray Crystallographic Study: All single-crystal X-ray experiments were performed on a Nonius CAD4 or Kappa CCD, or a Siemens P4 four-circle diffractometer. For example, with [GdCu₆], a crystal of dimensions 0.48 × 0.38 × 0.30 mm was mounted in a thin-

walled capillary for the structure determination. Intensity data were collected on a Siemens P4 diffractometer with Mo-K_α radiation in the ω-scan mode. Lattice parameter were obtained from a least-squares refinement of 36 reflections in the range 6.22° ≤ 2θ ≤ 33.14° and 2019 independent reflections were collected. Empirical absorption corrections were applied using the XPRED program. The structure was determined by direct methods and difference-Fourier syntheses, and refined by full-matrix least-squares using Siemens SHELXTL/PC system. The proton of the HL ligand in the complexes is assumed to have statistical distribution.

CCDC-135918 (C₂₄H₈₅Cl₂Cu₆GdN₆O₆₀), -135919 (C₂₄H₈₅Cl₂Cu₆N₆O₆₀Sm), -136464 (C₂₄H₈₅Cl₂Cu₆HoN₆O₆₀), and -170527 (C₂₄H₈₅Cl₂Cu₆N₆O₆₀Y) contain the supplementary crystallographic data for this paper. These data can be obtained free of charge at www.ccdc.cam.ac.uk/conts/retrieving.html [or from the Cambridge Crystallographic Data Centre, 12, Union Road, Cambridge CB2 1EZ, UK; fax: (internat.) +44-1223/336-033; E-mail: deposit@ccdc.cam.ac.uk].

Acknowledgments

This work was partly supported by the State Key Project of Fundamental Research (G1998061305), the National Science Fund for Distinguished Young Scholars (20125104) and NSFC (20023005), the Research Fund for the Doctoral Program of Higher Education (20010001020), and the Excellent Young Teachers Fund of MOE, P. R. C.

- [1] A. J. Blake, V. A. Cherepeno, A. A. Dunlop, C. M. Grant, P. E. Y. Milne, J. M. Rawson, R. E. P. Winpenny, *J. Chem. Soc., Dalton Trans.* **1994**, 2719–2727.
- [2] M. Andruh, I. Ramade, E. Codjovi, O. Guiliou, O. Kahn, J. C. Trombe, *J. Am. Chem. Soc.* **1993**, *115*, 1822–1829.
- [3] R. Georges, O. Kahn, O. Guiliou, *Phys. Rev.* **1994**, *B49*, 3235–3242.
- [4] M. Andruh, E. Bakalbassis, O. Kahn, J. C. Trombe, P. Porcher, *Inorg. Chem.* **1993**, *32*, 1616–1622.
- [5] C. Benelli, A. Caneschi, D. Gatteschi, O. Guiliou, L. Pardi, *J. Magn. Magn. Mater.* **1990**, *83*, 522–524.
- [6] C. Benelli, A. Caneschi, D. Gatteschi, O. Guiliou, L. Pardi, *Inorg. Chem.* **1990**, *29*, 1750–1755.
- [7] A. Bencini, C. Benelli, A. Caneschi, A. Dei, D. Gatteschi, *Inorg. Chem.* **1986**, *25*, 572–575.
- [8] A. Bencini, C. Benelli, A. Caneschi, R. L. Carlin, A. Dei, D. Gatteschi, *J. Am. Chem. Soc.* **1985**, *107*, 8128–8136.
- [9] S. W. Keller, V. A. Carson, D. Sandford, F. Stenzel, A. M. Stacy, G. H. Kwei, M. Alario-Franco, *J. Am. Chem. Soc.* **1994**, *116*, 8070–8076.
- [10] J. P. Costes, F. Dahan, A. Dupuis, J. P. Laurent, *Chem. Eur. J.* **1998**, *4*, 1616–1620.
- [11] O. Kahn, O. Guiliou, R. L. Oushoorn, M. Drillon, P. Rabu, K. Boubekeur, P. Batail, *New J. Chem.* **1995**, *19*, 655–660.

- [12] M. L. Kahn, C. Mathoniere, O. Kahn, *Inorg. Chem.* **1999**, *38*, 3692–3697.
- [13] Q. D. Liu, S. Gao, J. R. Li, Q. Z. Zhou, K. B. Yu, B. Q. Ma, S. W. Zhang, X. X. Zhang, T. Z. Jin, *Inorg. Chem.* **2000**, *39*, 2488–2492.
- [14] R. D. Willet, D. Gatteschi, O. Kahn, *Magneto-structural Correlations in Exchange Coupled Systems*; NATO ASI Series; D. Reidel Publishing Company: Dordrecht, Holland, **1985**.
- [15] H. Weihe, H. U. Güdel, *J. Am. Chem. Soc.* **1997**, *119*, 6539–6543.
- [16] O. Waldmann, J. Schülein, A. Koch, P. Müller, I. Bernt, R. W. Saalfrank, H. P. Andres, H. U. Güdel, P. Allenspach, *Inorg. Chem.* **1999**, *38*, 5879–5886.
- [17] G. L. Abbati, A. Cornia, A. C. Fabretti, W. Malavasi, L. Schenetti, A. Caneschi, D. Gatteschi, *Inorg. Chem.* **1997**, *36*, 6443–6446.
- [18] H. Weihe, H. U. Güdel, *J. Am. Chem. Soc.* **1997**, *119*, 6539–6543.
- [19] F. Le Gall, F. F. de Biani, A. Caneschi, P. Cinelli, A. Cornia, A. C. Fabretti, D. Gatteschi, *Inorg. Chim. Acta* **1997**, *262*, 123–132.
- [20] B. Pilawa, R. Desquiotz, M. T. Kelemen, M. Weickenmeier, A. Geisselmann, *J. Magn. Magn. Mater.* **1998**, *177–181*, 748–749.
- [21] A. Cornia, M. Affronte, A. G. M. Jansen, G. L. Abbati, D. Gatteschi, *Angew. Chem. Int. Ed.* **1999**, *38*, 2264–2266.
- [22] T. L. Jorris, M. Kozik, L. C. W. Baker, *Inorg. Chem.* **1990**, *29*, 4584–4586.
- [23] A. Müller, M. Penk, R. Rohlfing, E. Krickemeyer, J. Döring, *Angew. Chem. Int. Ed. Engl.* **1990**, *29*, 926–927.
- [24] A. Caneschi, A. Cornia, S. J. Lippard, *Angew. Chem. Int. Ed. Engl.* **1995**, *34*, 467–469.
- [25] A. Caneschi, A. Cornia, A. C. Fabretti, S. Foner, D. Gatteschi, R. Grandi, L. Schenetti, *Chem. Eur. J.* **1996**, *2*, 1379–1387.
- [26] D. M. J. Doble, C. H. Benison, A. J. Blake, D. Fenske, M. S. Jachson, R. D. Kay, W. S. Li, M. Schröder, *Angew. Chem. Int. Ed.* **1999**, *38*, 1915–1918.
- [27] K. Nakamoto, *Infrared Spectra of Inorganic and Coordination Compound*, 4th Ed., John Wiley & Sons Inc., New York, **1986**, 258.
- [28] A. Bouayad, C. Brouca-Cabarrecq, J. C. Trombe, *Inorg. Chim. Acta* **1992**, *195*, 193–201.
- [29] S. M. Bowen, E. N. Duesler, R. T. Paine, *Inorg. Chim. Acta* **1982**, *61*, 155–166.
- [30] J. G. Mao, L. Song, J. S. Huang, *J. Chem. Crystallog.* **1998**, *28*, 475–479.
- [31] J. G. Mao, L. Song, J. S. Huang, *Chin. J. Struc. Chem.* **1999**, *18*, 4–8.
- [32] L. J. Radonovich, M. D. Glick, *Inorg. Chem.* **1971**, *10*, 1463–1468.

Received June 21, 2002
[I02334]